AFM – Raman Characterization of Li-ion Batteries

Sergey Shashkov, [1,2] and Pavel Dorozhkin[2]
[1]Quantum Design, Japan
[2]NT-MDT Co., Moscow Russia

LITHIUM ION BATTERIES. INTRODUCTION

Development of advanced lithium batteries currently represents a very rapidly growing field of science and technology. Lithium batteries are interesting as a power source in numerous portable devices such as notebook computers, cellular phones and camcorders, in electrical vehicles, in military and aerospace applications.

Layered lithium cobalt oxide $LiCoO_2$ (Fig. 1) is the most commonly used cathode material in commercial lithium batteries. This is due to its longer cycle life, lower self-discharge rate and higher energy density compared to other rechargeable batteries (lead-acid, nickel cadmium or nickel metal hydride), higher cost effectiveness and smaller toxicity.

The layered form of $LiCoO_2$ has a rhombohedral symmetry with the cell parameters a=2.816 Å and c=14.09 Å [1]. Li and Co ions occupy alternate layers in octahedral sites between the close packed oxygen planes (Fig. 1).

$LiCoO_2$ structures have been extensively investigated, because such layered structures are perfectly suited to accommodate large changes of the Li content and provide the best pathway for Li^+ diffusion in and out of the lattice of crystal during the charge–discharge processes:

$$LiCoO_2 \underset{\text{Discharge}}{\overset{\text{Charge}}{\rightleftharpoons}} Li_{1-x}CoO_2 + xLi^+ + xe^-$$

During charging, lithium is de-intercalated from the cathode layers ($LiCoO_2$ cathode becomes delithiated, i.e. $Li_{1-x}CoO_2$), then transported and intercalated into the anode. During the discharge process, the lithium ions are de-intercalated from the anode, migrated across the electrolyte, and intercalated again to the empty octahedral site between layers in the cathode (deficit of Li is decreased and cathode transforms to $LiCoO_2$ again), the compensating electrons go to the external electrical circuit. Such a completely reversible lithium intercalation process is the key to the rechargeable Li battery. It is the ordinary process for any non-defective lithium battery.

Effects of protracted cycling (when charge and discharge cycles are repeated very often) or prolonged storing bring batteries away from their initial good performance.

With the course of time, a surface film consisting of variety of salts may be formed on the cathode or anode.

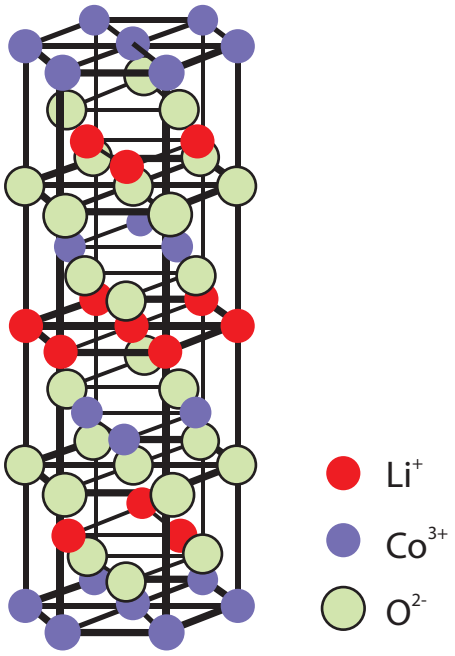

Fig. 1. Layered LiCoO2 structure.

It means that lithium ions must additionally travel through this new film. It may change the surface electrochemistry and lead to the unconventional charge/discharge chains.

There are also irreversible processes of electrolyte oxidation and reduction. Batteries can be overcharged with such circumstances; the cathode can undergo phase transformations. Microcrystals of $Li_{1-x}CoO_2$ ($0<x<0.1$) exist in the rhombohedral form with the cell parameters a=2.816 Å and c=14.09 Å. A little more de- lithiated $Li_{1-x}CoO_2$ ($0.45<x<0.57$) passes into a monoclinic structure. Upon further lithium extraction $Li_{1-x}CoO_2$ ($x>0.57$) enters the rhombohedrical form region again.

The c-axis of the crystal unit cell is increased from 14.09 Å to 14.26 Å, but the a-axis is decreased a bit (from 2.816 Å to 2.812 Å) at such transformation. As a result, the volume expansion of few percent is observed [1].

Phase transformations can lead to deterioration of electrical performance or even to degradation of cathode due to the mechanical strain, for example. Significant deformations in CoO_6 octahedrons and formation of Co_3O_4 / Li_2O can disrupt the intercalation / de-intercalation frameworks.

The formation of lithium oxide (Li_2O) inside batteries during prolonged cycling or storing according to the following reaction [2]

$$3LiCoO_2 + Li^+ + e^- = Co_3O_4 + 4Li_2O$$

can not be reversed electrochemically without destroying the battery. The cathode degrades through loss of Li2O and transforming $LiCoO_2$ into electrochemically inactive Co_3O_4.

Understanding distribution of degraded areas on the surface of a positive electrode is very important to improve life time of the batteries.

With the current trend of miniaturization and performance improvement, there is a need for knowledge of Li-ion batteries, Li intercalation and cathode degradation, on a sub-micron scale.

EXPERIMENTAL

Raman spectroscopy and atomic force microscopy (AFM) are valuable methods for the structural characterization of materials used as electrodes in rechargeable lithium batteries ($LiCoO_2$ in particular). In this note, we present results on a LiCoO cathode characterization measured by AFM and Raman techniques on the integrated instrument NTEGRA Spectra (NT-MDT) integrated with Renishaw inVia Raman spectrometer. The instrument allows simultaneous recording of various AFM and Raman images from the same sample area.

Typical structure of lithium-ion rechargeable cylindrical cell is shown on Fig. 2. The three primary functional components of a lithium-ion battery are the anode, cathode, and electrolyte. Carbonaceous material is used as an anode material (the most commercially popular anode material is graphite).

The inorganic compound, $LiCoO_2$, is used as the cathode material in the cylindrical cell. The electrolyte is a lithium salt in an organic solvent. The soft separators used in batteries must avoid direct contact between the anode and cathode, but they must allow a free transport of the electrolyte and lithium ions. The batteries typically have a nominal voltage around 3.7 volts.

Individual Lithium-ion ICR-18650 cylindrical cells from different laptop Lithium Battery Packs were investigated. The first battery pack was used for about 3 years, passed about 1200 charging/recharging cycles and had only about 25% of nominal capacity; the battery was ~30% charged. The second battery was new and ~65 % charged.

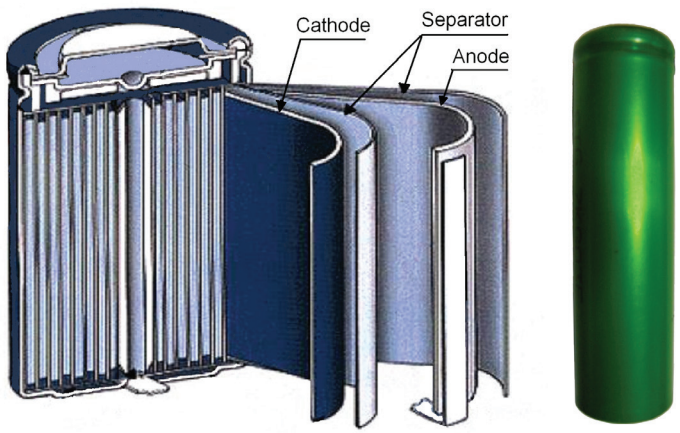

Fig. 2. Structure of Lithium-ion battery

Cylindrical cells were opened to separate the cathodes. Cathodes were immediately washed with anhydrous tetrahydrofuran and dried through the blotting paper after opening the cell. This procedure removed electrolyte salt from the electrode to prevent its reaction with moisture in air.

RESULTS

The surface morphology of $LiCoO_2$ cathode analyzed by AFM is presented in Fig. 3. AFM topography (Fig. 3a-b), provides information about size of grains, their shape and orientation. Lattice constants of cathode material are a function of the lithium concentration, x, in $Li_{1-x}CoO_2$ as described above. As a result, the surface of the new $LiCoO_2$ cathode is more smooth [3]; size of grains derived from the AFM topography images is ~2–2.5 µm. The used battery, cathode exhibits high roughness and grain structure; size of grains is ~2.5–3.5 µm. This is typical, due to the lithium extraction (in case of de-lithiated $LiCoO_2$), the crystal cell of $LiCoO_2$ is expanded and individual strained microcrystals of the cathode material may be observed on the surface.

Phase and magnitude of cantilever oscillation recorded during scanning provide complementary information to AFM topography. Phase imaging shows a clear contrast once there is a detectable variation of interaction forces between cantilever and surface. Thus, phase images highlight grain edges and are not affected by large-scale height differences providing clearer observation of the sample fine features (Fig. 3c-d). Magnitude (cantilever oscillation amplitude signal) provide additional contrast (Fig. 3e-f): grain edges are also clearly observed because control electronics does not respond instantaneously to the sharp changes in the sample height.

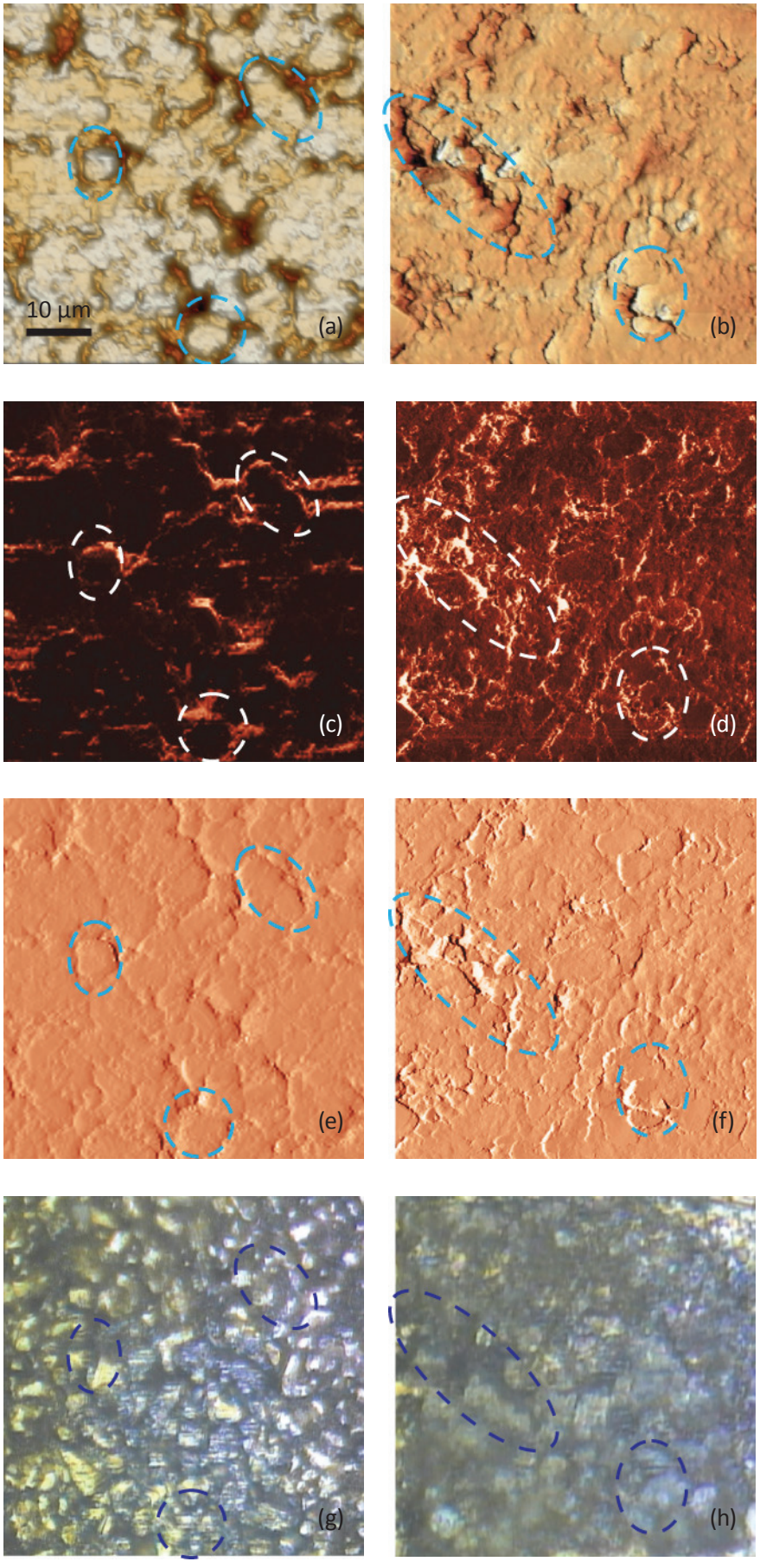

Fig. 3. AFM topography (a), (b), phase (c), (d), magnitude (e), (f) and optical images (g), (h) of the surface of $LiCoO_2$ cathodes from the used battery and from the new one. Pictures (a), (c) exhibit high roughness and grain structure which is typical for used batteries. Size of all images: 50x50 µm.

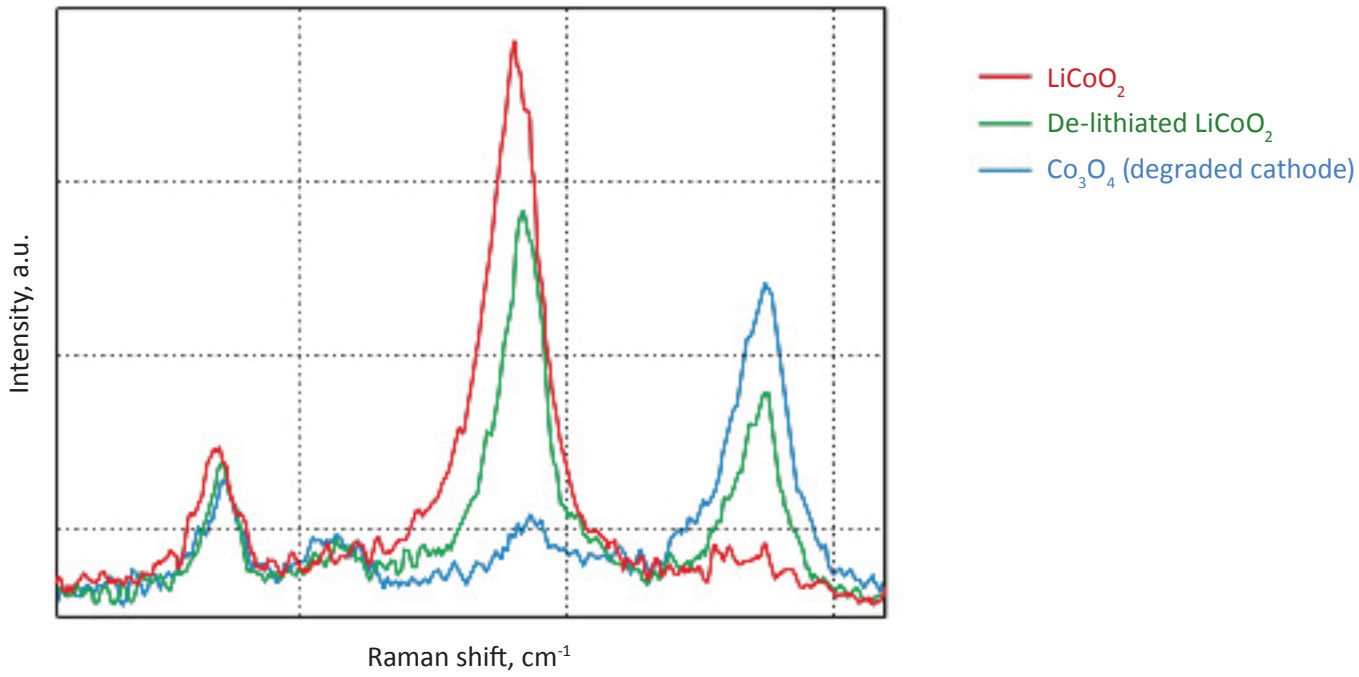

Fig. 4. Raman spectra of cathode: $LiCoO_2$ (red), de-lithiated $LiCoO_2$ (green), and Co_3O_4 (blue). The resolved bands may be related with the structural distortion or the surface change during the extraction of Li.

Optical images give complementary information to the AFM measurements. There is not complete correlation between the optical and AFM images (Fig. 3). Optical images of the cathode are formed by reflected light that is sensitive to the nature of the interface and grain reflection properties. The amount of light reflected back to the video CCD depends on crystal surface orientation.

Raman spectra of the $LiCoO_2$ cathode depend on the electrochemical history. From different points on the cathode (Fig. 3) different spectra can be observed (Fig. 4).

By factor group analysis, the total irreducible representation for the vibrational modes of $LiCoO_2$ is obtained as $A_{1g} + 2A_{2u} + E_g + 2E_u$. The gerade modes are Raman active and the ungerade modes are IR active. Only two bands should be observed in Raman spectra of $LiCoO_2$: $A_{1g} + E_g$. In fact, experimental spectra of LiCoO exhibit two strong bands at 472 cm^{-1} and 579 cm^{-1} with the intensity ratio of 1:3 (red spectrum on Fig. 4), which correspond to oxygen vibrations involving v2 (E_g), O-Co-O bending, and v1 (A_{1g}), Co-O stretching modes, respectively (Fig. 5). In the A_{1g} mode two oxygen atoms vibrate in the opposite directions parallel to the c-axis of $LiCoO_2$, while in the Eg mode they vibrate in the opposite directions parallel to the Co atom planes [4] (Fig. 5). The positions of these peaks and their intensity are very sensitive to the long- range order in CoO_2 slabs.

Upon the extraction of lithium from the cathode (during battery charging process), some changes are observed in the Raman spectra (green spectrum in Fig. 4). The intense peaks of the LiCoO (472 cm^{-1} and 579 cm^{-1} bands) experience a small spectral shift. Intensity of 515 cm^{-1} and 674 cm^{-1} bands is increased. The peak centered at 674 cm^{-1} (blue spectrum in Fig. 4) may be assigned to a mode vibration of Co_3O_4 species; the peak at 515 cm^{-1} may be assigned to a mode vibration of Li_2O.

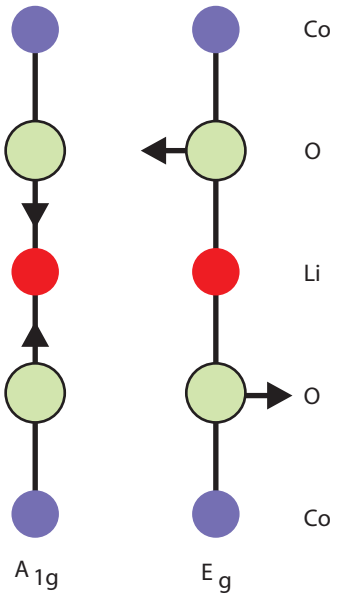

Fig. 5. Atomic displacements of the Raman-active modes of $LiCoO_2$

We can distinguish the next regularity in the Raman spectra of lithium battery cathode:

1. areas of the cathode in the intercalated state ($LiCoO_2$) are characterized by two intense peaks at 472 cm^{-1} and 579 cm^{-1} (red spectrum in Fig. 4);
2. de-lithiated cathode, ($Li_{1-x}CoO_2$) is characterized by comparable intensities of Raman bands at 579 cm^{-1} and 674 cm^{-1} (green spectrum in Fig. 4);
3. degraded areas of cathode (Li_2O is lost completely at such areas, and $LiCoO_2$ is transformed into the electrochemically inactive Co_3O_4) are characterized by a strong peak at 674 cm^{-1} and almost complete disappearance of the peak at 579 cm^{-1} (blue spectrum in Fig. 4).

Two dimensional Raman and AFM maps from the same place of the cathode removed from the new battery pack are depicted in Fig. 6a-g (see Fig. caption for description).

Data in Fig. 6d-f represents chemical composition of the cathode. Charged areas (places with deficit of Lithium ions, i.e. de-lithiated or de-intercalated areas) are shown in green in Fig. 6e-f. Red color (Fig. 6d, 6f) represents discharged areas of the cathode (i.e. the intercalated state). More quantitative data about lithium intercalation can be derived from the ratio of 579 cm^{-1} and 674 cm^{-1} peaks (Fig. 6g).

Bright places on the figure correspond to the parts of cathode in the intercalated state ($LiCoO_2$), because at those places the peak at 579 cm^{-1} is strong, while the peak at 674 cm^{-1} is weak (as result, the ratio of intensities at such features is large and reaches the value of 8 - almost completely intercalated state).

Dark areas of cathode in Fig. 6g can be assigned to the de-intercalated cathode ($Li_{1-x}CoO_2$). Peak intensity of 674 cm^{-1}

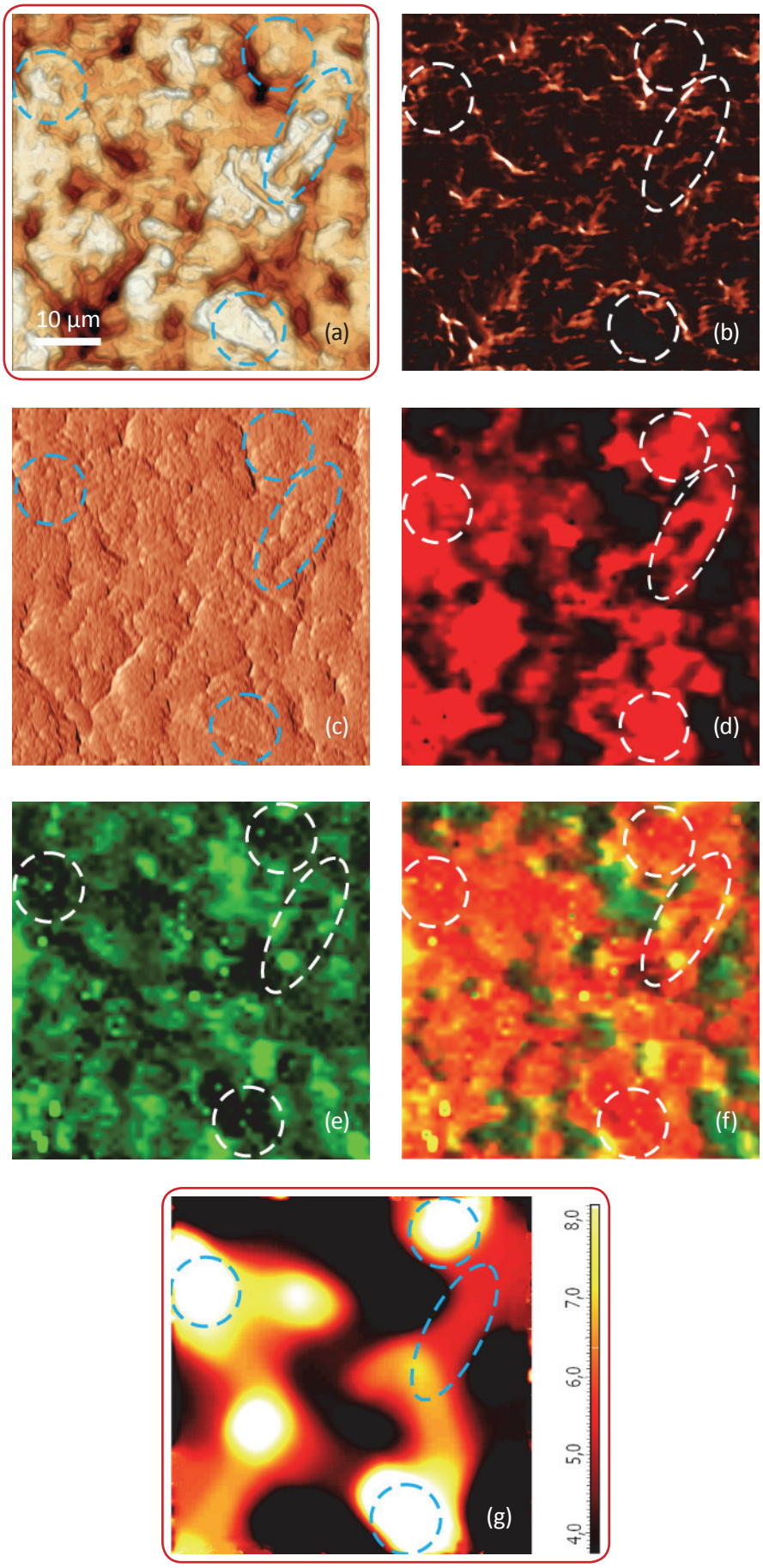

Fig. 6. AFM and Raman images from the same place of the new cathode: (a) AFM topography Height, (b) Phase, (c) Mag; (d) Raman intensity map with 579 cm^{-1} peak, (e) Raman intensity map using 674 cm^{-1} peak; (f) chemical map (red color corresponds to the $LiCoO_2$, green color is delithiated $LiCoO_2$ (Co3O4 are absent on this cathode, because the intensity of peak at 674 cm^{-1} is never rank over the intensity of peak 579 cm); (f) ratio of peak intensities at 579 and 674 cm^{-1}. Black color corresponds to the delithiated cathode, yellow color corresponds to the intercalated state of cathode. Size of all images: 50x50 µm.

band at such areas is sufficiently strong, but it never exceeds intensity of the peak at 579 cm^{-1}. It is a sign, that the cathode from the unused battery does not have any degraded areas (Co_3O_4 species) at all.

Bright areas in Fig. 6d and dark areas in Fig. 6e (intercalated cathode area) correlate with the intense features in Fig. 6g. The corresponding areas of cathode can be observed on AFM images (Fig. 6a-c). Topographical information (surface morphology) is directly related to the cathode chemical state derived from the Raman spectra. Some of topographical features in Fig. 6a-c related to the intercalated $LiCoO_2$ and marked with the ovals are in accordance with Fig. 6g. In general, higher areas on the AFM topography correspond to the more intercalated state of the cathode.

The area of cathode relevant to the de-lithiated material is 60 % approximately (Fig. 6f-g). This is in accordance with the charge level of battery (it was ~65 % charged).

Raman images of cathode removed from the used battery pack are more complicated. (Fig. 7a-g).

Such cathode has degraded Co_3O_4 areas in addition. Surface of cathode from the used battery pack consists of many areas, which can be characterized by the strong peak at 674 cm^{-1} and almost completely disappeared peak at 579 cm^{-1} (the ratio of intensities at such features is very small) Black areas in Fig. 7g may be assigned to the degraded parts of the cathode (Co_3O_4). These areas are blue in Fig. 7e-f. The bright areas in Fig. 7g indicate that some of the part of cathode is not degraded (red color in Fig. 7d, 7f). The topographical features in Fig. 7a-c marked with oval are related to the non degraded cathode (Fig. 7g). The larger ratio of intensities at 579 cm^{-1} and 674 cm^{-1} is a sign that those areas of the cathode are more intercalated.

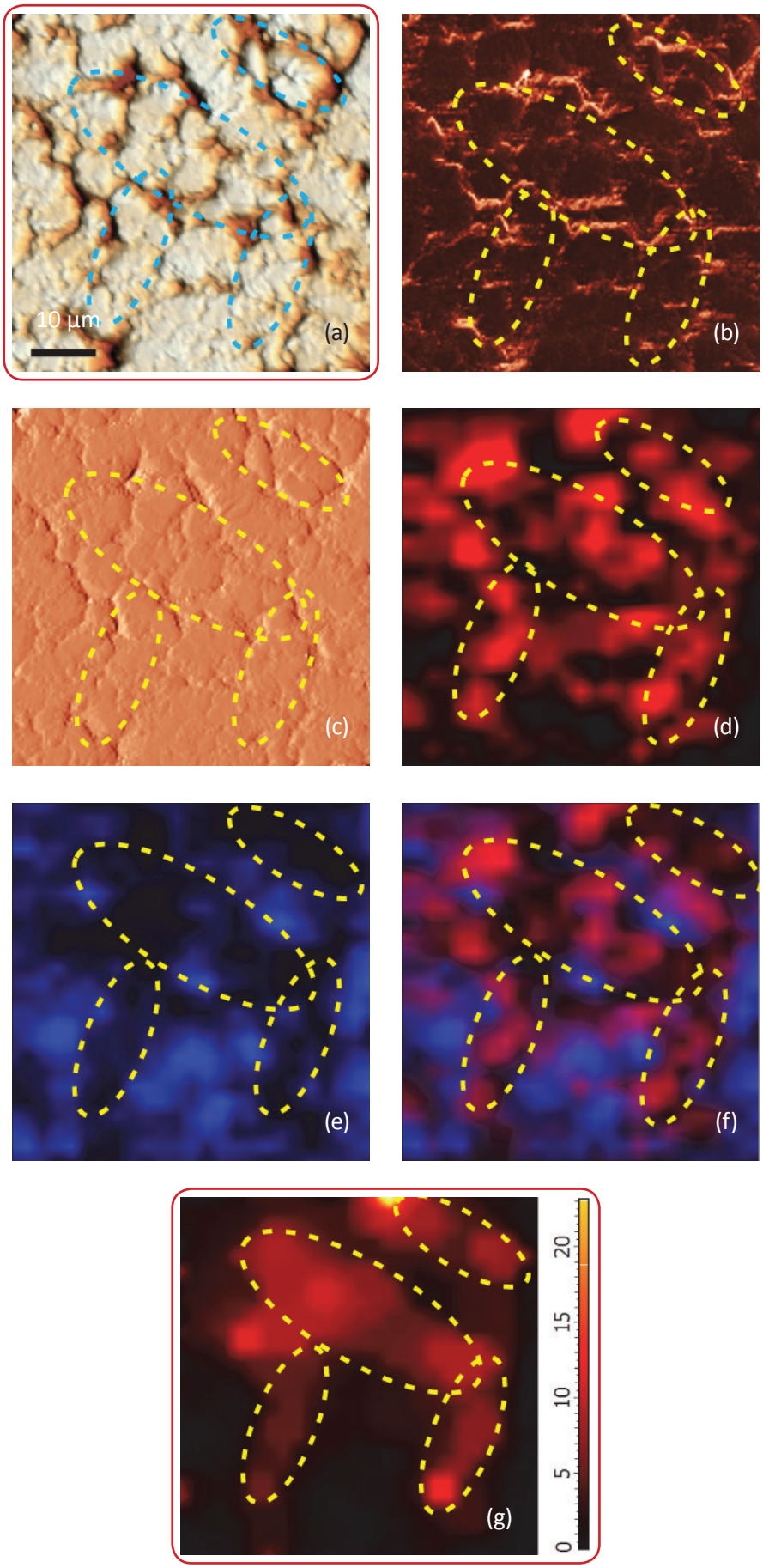

Fig. 7. AFM and Raman images from the same place of cathode removed from the old battery: (a) AFM topography, (b) Phase, (c) Magnitude; (d) Raman intensity map using 579 cm^{-1} peak, (e) Raman intensity map using 674 cm^{-1} peak; (f) ratio of peak intensities at 579 cm^{-1} and 674 cm^{-1}. Black color corresponds to the Co_3O_4, because such areas are characterized by a strong peak at 674 cm^{-1} and very weak peak at 579 cm^{-1}; (g) chemical map (blue color corresponds to the Co_3O_4, red color corresponds to the non degraded $LiCoO_2$. Size of all images: 50x50 µm.

Comparing Raman map (Fig. 7g) with AFM topography (Fig. 7a) reveals that non degraded parts of the cathode correspond to areas with higher amount of smaller grains and larger amount of grain boundaries (shown by ovals in the Fig. 7). At the same time, areas with the degraded cathode (outside of oval areas) show more flat topography with larger grains and less grain boundaries.

CONCLUSION

This study has demonstrated the importance of correlated AFM-Raman imaging for Li-ion battery studies. Raman imaging allows to characterize in details lithium intercalation processes and degradation of the cathode. Simultaneous AFM imaging allows one to correlate cathode chemical properties with its topography (roughness, grain structure etc.).

ACKNOWLEDGEMENT

NT-MDT is grateful to Renishaw K.K. (Tokyo) for providing inVia Raman spectrometer for the integrated AFM-Raman instrument used in this work.

REFERENCES

[1] J. N. Reimers, J. Dahn, J. Electrochem. Soc, 139 ,8 (1992) 2091.
[2] E. Markevich, G. Salitra, D. Aurbach, Electrochem. Commun. 7 (2005) 12981304.
[3] Y. Park, Nam Hoon Kim, Ja Young Kim, In-Yong Eom, Yeon Uk Jeong, Min Soo Kim, Sung Man Lee, Hyun Chul Choi, Young Mee Jung, Vibrational Spectroscopy 53 (2010) 6063.
[4] Kazunory Ozawa, Lithium Ion Rechargeable batteries: Materials, technology, and new application, Wiley-VCH Verlag GmbH&Co, Weinheim, 2009.